Journal of proteome research

pubs.acs.org/jpr Article

Profiling Glycosylphosphatidylinositol (GPI)-Interacting Proteins in the Cell Membrane Using a Bifunctional GPI Analogue as the Probe

Sayan Kundu,[‖] Chuwei Lin,[‖] Mohit Jaiswal,[‖] Venkanna Babu Mullapudi, Kendall C. Craig, Sixue Chen, and Zhongwu Guo*

Cite This: *J. Proteome Res.* 2023, 22, 919−930 Read Online

ACCESS | Metrics & More | Article Recommendations | Supporting Information

ABSTRACT: Glycosylphosphatidylinositol (GPI) anchorage of cell surface proteins to the membrane is biologically important and ubiquitous in eukaryotes. However, GPIs do not contain long enough lipids to span the entire membrane bilayer. To transduce binding signals, GPIs must interact with other membrane components, but such interactions are difficult to define. Here, a new method was developed to explore GPI-interacting membrane proteins in live cell with a bifunctional analogue of the glucosaminylphosphatidylinositol motif conserved in all GPIs as a probe. This probe contained a diazirine functionality in the lipid and an alkynyl group on the glucosamine residue to respectively facilitate the cross-linkage of GPI-binding membrane proteins with the probe upon photoactivation and then the installation of biotin to the cross-linked proteins via a click reaction for affinity-based protein isolation and analysis. Profiling the proteins pulled down from the Hela cells revealed 94 unique and 18 overrepresented proteins compared to the control, and most of them are membrane proteins and many are GPI-related. The results have proved not only the concept of using the new bifunctional GPI probe to investigate GPI-binding membrane proteins but also the important role of inositol in the biological functions of GPI anchors and GPI-anchored proteins.

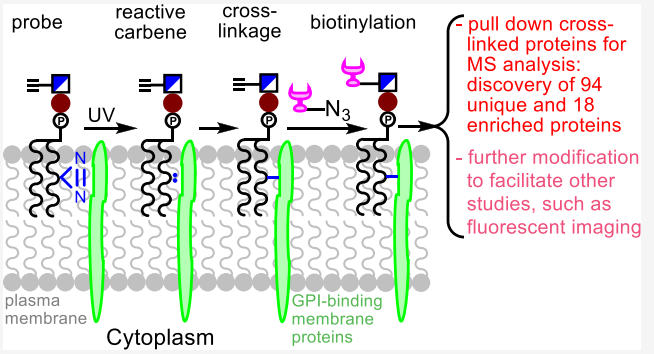

KEYWORDS: *glycosylphosphatidylinositol (GPI), GPI-interacting protein, photoactivated cross-linking, diazirine, alkyne, proteomics*

INTRODUCTION

Cell membrane-associated biomolecules connect cells and the extracellular matrix (EM), and their interactions with molecules outside of the cell regulate numerous cellular activities.[1] Among various types of membrane-associated molecules, glycosylphosphatidylinositol-anchored proteins (GPI-APs) occupy a unique niche.[2] GPI-APs are generated by the covalent linkage of GPIs, a class of complex glycolipids, to the protein C-terminus (Figure 1), representing one of the most common and important posttranslational modifications.[3,4] GPI biosynthesis, as well as its linkage form with proteins, is highly conserved from single-cell protozoa to vertebrates.[5,6]

GPI-APs are ubiquitous in eukaryotes and have been discovered in different species and cells. GPI-APs are associated with the cell membrane through embedding the lipid tails of GPIs in the membrane lipid bilayer (Figure 1). As an integral part of the cell membrane, GPI-APs play a key role in various physiological and pathological processes,[7,8] especially in signal transduction.[9,10] For example, GPI-APs are regulators of synapse development,[11] and CD59 is a transducer of T cell activation signal and protects cells against complement-induced lysis.[12] GPI-APs also function as molecular chaperons and coreceptors.[13] Furthermore, it has been disclosed that the GPI moiety has a significant influence on the distribution of GPI-APs in the cell membrane and related signaling events.[14−18] For instance, substituting the GPI anchor in Thy-1 with a transmembrane polypeptide domain results in significant changes in its functions,[17] and altering the GPI anchor moiety of the prion protein (PrP^c) affects its activation and trafficking.[19] The functional specificity imposed to proteins by GPI anchors is disclosed to depend on the tenancy of GPI anchors to be preferentially present in some specific microdomains of the cell membrane.[20] Thus, GPIs function far beyond as an anchoring system but are directly involved in various biological processes.

However, the lipid chains of GPIs are usually not long enough to span the entire lipid bilayer of the cell membrane. Therefore, GPIs need to interact with other cell membrane

Received: November 10, 2022
Published: January 26, 2023

https://doi.org/10.1021/acs.jproteome.2c00728
J. Proteome Res. 2023, 22, 919−930

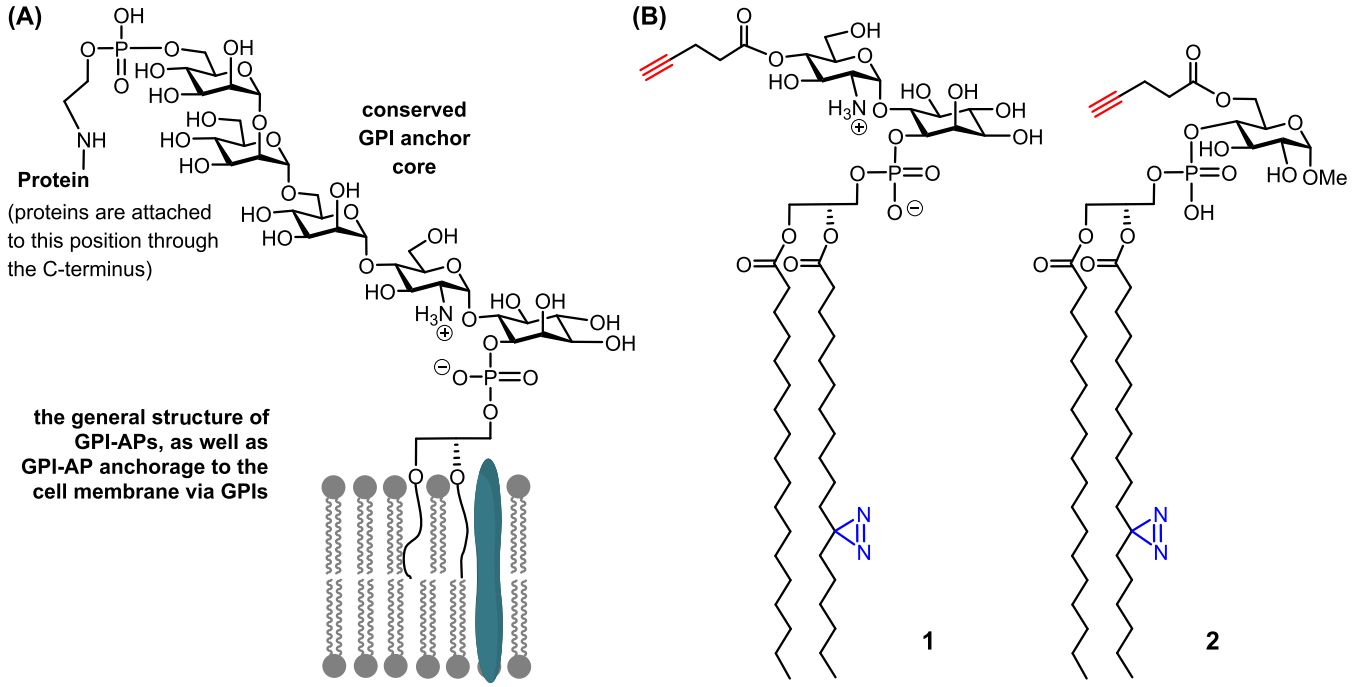

Figure 1. (A) Representative structure of GPI-APs, as well as schematic illustration of GPI-AP attachment to the cell membrane, and (B) the structures of probe **1** used to study GPI−cell membrane interactions and glycolipid **2** used as a negative control.

components to transduce transmembrane signals. Some studies have revealed that GPIs can selectively interact with lipids in specific microdomains of the cell membrane,[21] whereas other studies show that GPI anchors may associate with transmembrane proteins to relay interacting signals.[22] For example, various GPI-APs, such as CD55, CD59, CD48, and Thy-1, are associated with the Src family of protein tyrosine kinases to accomplish signal transduction.[18] Despite the general acknowledgment of transmembrane protein involvement in GPI signaling, currently, there is a lack of understanding about these proteins and related pathways because systematic studies on GPI−protein interactions remain challenging. Therefore, finding out the protein partners of GPIs in the membrane is crucial because it not only uncovers the signaling pathways of GPI-APs but also helps identify novel molecular markers useful for drug development. This work aims to establish a method to address this issue and perform proof-of-concept studies.

MATERIALS AND METHODS

General Methods

All chemicals were of analytical grades obtained from commercial sources and used without further purification unless specified otherwise. Molecular sieves 4A were flame-dried under high vacuum and used immediately after being cooled to rt under N_2. Analytical TLC was performed using silica gel 60 Å F254 plates detected by an ultraviolet (UV) detector and/or by charring with 10% (v/v) H_2SO_4 in ethanol. Flash column chromatography was performed with silica gel 60 (230−400 mesh). NMR spectra were acquired using a 600 MHz machine with chemical shifts reported in ppm (δ) referenced to CD_3OD (^{1}H NMR δ 3.31 ppm, ^{13}C NMR δ 49.0) or $CDCl_3$ (^{1}H NMR δ 7.26 ppm, ^{13}C NMR δ 77.0 ppm). Peak and coupling constant assignments are made based on ^{1}H NMR, ^{1}H−^{1}H COSY, and ^{1}H−^{13}C heteronuclear single-quantum correlation (HSQC) experiments. High-resolution electrospray ionization-time of flight mass spectra (HR ESI-TOF MS) of the synthetic compounds were acquired with a Waters Xevo G2-XS QTof instrument in the positive mode. Paraformaldehyde, copper(II) sulfate, poly-L-lysine, tris(2-carboxyethyl) phosphine hydrochloride (TCEP), and sodium ascorbate were purchased from Sigma Aldrich. Fetal bovine serum (FBS), Dulbecco's modified Eagle's medium (DMEM), and the penicillin−streptomycin solution were purchased from ATCC. 4′,6-Diamidino-2-phenylindole (DAPI), Dulbecco's phosphate buffer saline (DPBS), and streptavidin agarose resin (pierce streptavidin agarose) were purchased from Thermo Fisher scientific. THPTA (tris-hydroxypropyltriazolylmethylamine), Cy5-azide, and biotin-azide (Biotin-PEG3-Azide) were purchased from Click Chemistry Tools. RPMI 1640 media was purchased from Lonza. Streptavidin-Cy5 was purchased from Abcam. Fluorescent imaging was performed using an Olympus IX71 inverted system equipped with a light-emitting diode (LED) light source (Cool LED, PE-300), 20 × 0.8 NA and 40 × 1.4 NA plan apochromatic objectives (Olympus LUCPlanFl N objective), DAPI and Cy5 fluorescence channels, and Olympus DP23M color camera. Image analysis was performed using Olympus Cellsens Standard 3 software and FIJI/ImageJ software. Probe **1** was synthesized according to our previous report.[23] The cell lysis buffer contained 4% sodium dodecyl sulfate (SDS), 120 mM NaCl, and 50 mM triethanolamine.

Synthesis of Methyl 2,3-di-*O*-(*para*-Methoxybenzyl)-6-*O*-(4-pentynoyl)-α-D-glucopyranoside (7). A solution of *N*,*N*′-dicyclohexylcarbodiimide (DCC, 142.4 mg, 0.69 mmol), 4-pentynoic acid (47.4 mg, 0.48 mmol), and 4-dimethylaminopyridine (DMAP, 11.2 mg, 0.092 mmol) in CH_2Cl_2 and tetrahydrofuran (THF) (1:1, 6 mL) was cooled to 0 °C and stirred for 30 min. Then, diol **6** (200.0 mg, 0.46 mmol) was added and the reaction mixture was stirred at rt overnight. The reaction mixture was filtered to remove the urea byproduct, and the filtrate was diluted with CH_2Cl_2 (30 mL) and washed

https://doi.org/10.1021/acs.jproteome.2c00728
J. Proteome Res. 2023, 22, 919−930

with aqueous $NaHCO_3$ solution and brine. The organic layer was dried over Na_2SO_4 and concentrated in vacuum. The residue was applied to silica gel column chromatography to get **7** (180 mg, 76%) as colorless syrup. R_f = 0.35 (40% EtOAc in Hex). ^{1}H NMR (600 MHz, $CDCl_3$): δ 7.36−7.30 (m, 4 H), 6.89−6.86 (m, 4 H), 4.92 (d, J = 11.0 Hz, 1 H), 4.73 (d, J = 11.9 Hz, 1 H), 4.66 (d, J = 11.0 Hz, 1 H), 4.61 (d, J = 11.9 Hz, 1 H), 4.55 (d, J = 3.6 Hz, 1 H, Glc-1), 4.41 (dd, J = 5.2, 11.2 Hz, 1 H, Glc-6), 4.29 (dd, J = 2.2, 12.0 Hz, 1 H, Glc-6′), 3.80 (s, 3 H), 3.79 (s, 3 H), 3.76−3.70 (m, 2 H, Glc-3, Glc-5), 3.47 (dd, J = 3.6, 9.6 Hz, 1 H, Glc-2), 3.41−3.39 (m, 1 H, Glc-4), 3.37 (s, 3 H), 2.60−2.55 (m, 2 H), 2.51−2.46 (m, 2 H), 1.96 (t, J = 2.6 Hz, 1 H, alkyne C−H). ^{13}C[^{1}H] NMR (150 MHz, $CDCl_3$): δ 171.8 (C═O), 159.4, 159.3, 130.7, 130.0, 129.7 (2 C), 129.6 (2 C), 113.9 (2 C), 113.8 (2 C), 98.2 (Glc-1), 82.3, 80.7 (Glc-3), 79.0 (Glc-2), 75.0, 72.8, 69.8 (Glc-4), 69.1 (2 C, Glc-5, alkyne terminal C), 63.5 (Glc-6), 55.2 (3 C, 3 OMe), 33.1, 14.2. HR ESI-TOF MS: calcd for m/z $C_{28}H_{38}NO_9$ [M + NH_4]$^+$, 532.2541; found, 532.2539.

Synthesis of Methyl 4-*O*-[2-Cyanoethanol (*R*)-2-*O*-[11-(3-hexyl-3*H*-diazirin-3-yl)undecanoyl]-3-*O*-stearoyl-glycerol phosphoryl]-2,3-di-*O*-(*para*-methoxybenzyl)-6-*O*-(4-pentynoyl)-α-D-glucopyranoside (9). To a solution of **7** (50.0 mg, 0.097 mmol), molecular sieves 4A (100.0 mg), and tetrazole (0.45 M in acetonitrile, 2.1 mL, 0.97 mmol) in anhydrous CH_2Cl_2/CH_3CN (3:1, 8 mL) was slowly added a solution of freshly prepared phosphoramidite **8** (330.0 mg in 1 mL of dry CH_2Cl_2, 0.39 mmol) under an Ar atmosphere at rt, and the mixture was stirred for 30 min. Then, it was cooled to −40 °C, which was followed by the addition of *tert*-butyl hydroperoxide (5.5 M in decane, 353 μL, 1.94 mmol). The mixture was stirred at −40 °C for 1 h, and Me_2S (215 μL, 2.92 mmol) was added. The mixture was stirred at −40 °C for another 1 h, poured into saturated aqueous $NaHCO_3$ solution, and extracted with CH_2Cl_2 (3 × 50 mL). The combined organic layers were dried over Na_2SO_4 and concentrated in vacuum. The product was purified by silica gel column chromatography to afford **9** (85 mg, 68%, ∼1:1 mixture of diastereomers) as a colorless syrup. R_f = 0.2 (40% EtOAc in Hex). ^{1}H NMR (600 MHz, $CDCl_3$): δ 7.32−7.25 (m, 8 H), 6.89−6.85 (m, 8 H), 5.20−5.19 (m, 1 H, Gly-2), 5.05−5.03 (m, 1 H), 5.00 (d, J = 10.6 Hz, 1 H), 4.95 (d, J = 10.6 Hz, 1 H), 4.71−4.67 (m, 2 H), 4.64 (d, J = 10.5 Hz, 1 H), 4.57 (dd, J = 6.6, 12.0 Hz, 2 H), 4.53 (d, J = 3.4 Hz, 1 H, Glc-1), 4.51 (d, J = 3.4 Hz, 1 H, Glu-1), 4.40−4.36 (m, 2 H, Glc-6), 4.32−4.25 (m, 5 H, Glc-4, Glc-6′), 4.19−3.96 (m, 10 H), 3.94−3.88 (m, 6 H, Glc-3, Glc-5), 3.81 (s, 3 H), 3.80 (s, 9 H), 3.54−3.51 (m, 2 H, Glc-2), 3.37 (s, 6 H), 2.64−2.59 (m, 4 H), 2.52−2.50 (m, 4 H), 2.32−2.25 (m, 10 H), 1.95 (bs, 2 H, acetylene C-H), 1.61−1.57 (m, 8 H), 1.35−1.33 (m, 8 H), 1.29−1.21 (m, 92 H), 1.10−1.03 (m, 8 H, α-CH_2 of diazirine), 0.89−0.87 (m, 12 H, CH_3). ^{13}C[^{1}H] NMR (150 MHz, $CDCl_3$): δ 173.2 (C═O), 173.1 (C═O), 172.8 (2 C, C═O), 171.5 (C═O), 171.4 (C═O), 159.6 (2 C), 159.1 (2 C), 130.6, 130.4, 129.8 (4 C), 129.7 (2 C), 129.2 (2 C), 128.9 (2 C), 116.4, 116.2, 113.9 (4 C), 113.7 (4 C), 97.9 (2 C, Glc-1), 82.5 (2 C), 79.3 Glc-2, 79.2, 78.9 (2 C, Glc-3), 78.8 (2 C), 75.6 (Glc-4), 74.8, 74.7, 73.1, 73.0, 69.2 (alkyne terminal C), 69.0 (2 C, Gly-2), 67.9 (Glc-5), 67.8, 66.2, 66.0, 65.9 (2 C), 62.6, 62.5, 62.4, 62.1 (2 C), 61.6, 61.5, 55.2 (2 C), 55.3, 55.2 (3 C), 45.1, 34.1, 34.0, 33.9, 33.0 (2 C), 32.9 (3 C), 31.9 (3 C), 31.6 (2 C), 29.7 (16 C), 29.6, 29.5, 29.4 (2 C), 29.3 (3 C), 29.2 (2 C), 29.1, 29.0, 28.9, 24.8 (2 C), 23.8 (2 C), 22.7, 22.5, 19.4, 19.1, 14.2 (2 C), 14.1, 14.0. ^{31}P[^{1}H] NMR (243 MHz, $CDCl_3$): δ −2.0, −2.6. HR ESI-TOF MS: calcd for m/z $C_{70}H_{114}N_4O_{16}P^+$ [M + NH_4]$^+$, 1297.7962; found, 1297.7986.

Synthesis of Methyl 4-*O*-[(*R*)-2-*O*-[11-(3-Hexyl-3*H*-diazirin-3-yl)undecanoyl]-3-*O*-stearoyl-glycerol phosphoryl]-6-*O*-(4-pentynoyl)-α-D-glucopyranoside (2). To the solution of **9** (12.0 mg, 9.0 μmol) in CH_2Cl_2 (300 μL) were added two drops of 1,8-diazabicyclo [5.4.0] undec-7-ene (DBU), and the solution was stirred at rt for 1 h. Trifluoroacetic acid (TFA) in CH_2Cl_2 (20%, 300 μL) was added to the reaction mixture to give a final concentration of ∼10% TFA. After stirring at rt for 30 min, the reaction was co-evaporated with toluene five times, and the product was purified by silica gel column chromatography to give **2** (7.3 mg, 79%) as an off-white solid. R_f = 0.4 (15% MeOH in $CHCl_3$). ^{1}H NMR (600 MHz, CD_3OD:$CDCl_3$, 1:2): δ 5.23−5.21 (m, 1 H, Gly-2), 4.73 (d, J = 3.6 Hz, 1 H, Glc-1), 4.50 (bd, J = 11.6 Hz, 1 H, Glc-6′), 4.40−4.39 (m, 1 H), 4.21 (dd, J = 6.8, 12.0 Hz, 1 H, Glc-6), 4.17 (dd, J = 6.0, 12.0 Hz, 1 H), 4.05−3.99 (m, 2 H), 3.98−3.91 (m, 1 H, Glc-4), 3.83−3.86 (m, 2 H, Glc-3, Glc-5), 3.54 (dt, J = 3.0, 9.6 Hz, 1 H, Glc-2), 3.42 (s, 3 H), 2.62−2.59 (m, 2 H), 2.52 (m, 2 H), 2.50−2.48 (m, 2 H), 2.33−2.30 (m, 4 H), 2.05 (t, J = 2.6 Hz, 1 H, acetylene C−H), 1.61−1.58 (m, 4 H), 1.36−1.22 (m, 50 H), 1.08−1.02 (m, 4 H, α-CH_2 of diazirine), 0.89−0.86 (m, 6 H, CH_3); ^{13}C[^{1}H] NMR (CD_3OD:$CDCl_3$, 1:2, 150 MHz): δ 174.5 (C═O), 174.2 (C═O), 172.5 (C═O), 99.9 (Glc-1), 82.9, 74.7 (Glc-4), 74.2 (Glc-3), 72.1 (Glc-2), 71.0 (Gly-2), 69.8 (Acetylene terminal C), 69.1 (Glc-5), 64.6, 64.3 (Glc-6), 63.1, 55.8, 34.8, 34.7, 33.8, 33.5, 32.5, 32.2, 30.3 (3 C), 30.1 (3 C), 30.0 (7 C), 29.9 (2 C), 29.8 (2 C), 29.7, 29.5, 25.5 (2 C), 24.5, 24.4, 23.2, 23.0, 14.8, 14.5, 14.4. ^{31}P[^{1}H] NMR (243 MHz, $CDCl_3$): δ −2.4. HR ESI-TOF MS: calcd for m/z $C_{51}H_{95}N_3O_{14}P^+$ [M + NH_4]$^+$, 1004.6546; found, 1004.6561

Cell Culture

Hela cells were cultured in high-glucose DMEM supplemented with 10% (v/v) FBS, 100 μg/mL streptomycin, and 100 U/mL penicillin. The cells were grown in a 5% CO_2 incubator maintaining a water-saturated atmosphere at 37 °C. For various biochemical studies, Hela cells of four passages were used.

Fluorescence Imaging of Probe-Treated Hela Cells

Hela cells (50 × 10^3) were seeded onto poly-L-lysine (1% solution in DPBS)-coated 35 mm dish and were allowed to grow to ∼60% confluence. The cells were washed three times with DPBS and then incubated with 1 mL of RPMI buffer containing 10 μM probe **1** (5.7 μL from 1.76 mM stock solution in DMSO) or **2** (4.5 μL from 2.23 mM stock solution in DMSO), respectively. For the negative control, the cells were incubated with DPBS only. After 4 h of incubation, the cells were washed with DPBS three times, and then 1 mL of DPBS was added to each dish. The cells were exposed to UV irradiation (365 nm wavelength) for 15 min using a Spectroline UV lamp at 4 °C (Spectroline, ENF-280C, 120 V, 60 Hz, 0.20 Amps), which was followed by washing. The cells were then incubated with 4% paraformaldehyde (PFA) in DPBS and rinsed with DPBS (3 × 1 mL). The fixed cells were incubated with click master mix (10 μM Biotin-Azide, 100 mM THPTA, 100 mM sodium ascorbate, and 15 mM $CuSO_4$) at rt for 1 h as described in the literature.[24] The cells were washed with DPBS (3 × 500 μL), 500 mM aq. NaCl solution (3 × 500 μL), and then deionized (DI) water. The cells were incubated

https://doi.org/10.1021/acs.jproteome.2c00728
J. Proteome Res. 2023, 22, 919−930

with streptavidin-Cy5 (1:1000 dilution of 1 mg/mL stock) in 1 mL of DPBS for 30 min in the dark. After washing with DPBS, the cells were incubated with DAPI (50 nM, 1 mL for each dish) at rt for 5 min. Finally, the cells were washed three times with DPBS and subjected to fluorescent imaging.

Labeling Proteins of Live Hela Cells with Probes 1 and 2

Hela cells (0.8×10^6) were seeded onto a 100 mm tissue culture dish as mentioned above and were allowed to grow up to 90% confluence. The cells were harvested, pelleted, and resuspended in 7 mL of serum-free media with a final cell count of about 4.7×10^6. The cells were equally divided into three centrifuge tubes, washed with DPBS three times, replenished with fresh serum-free media containing 200 μM of a probe or PBS (the negative control), and then transferred onto 35 mm tissue culture dish. Following incubation at 37 °C for 4 h, the cells were washed with DPBS, resuspended in 1 mL of DPBS, and exposed to 365 nm UV light as described above. Thereafter, the cells were pelleted through centrifugation (800*g*, 6 min, 4 °C) and washed with cold DPBS (2×) and aspirated. Cell pellets were either stored at −80 °C until use or directly applied to the next step.

Western Blot Analysis of Labeled Proteins

This experiment followed the reported protocols.[25,26] Cell pellets obtained above were lysed in lysis buffer (500 μL) containing 5.0 μL of protease inhibitor (Halt protease inhibitor cocktail, Thermo Scientific) on a Qsonica probe sonicator (6 pulses, 60% duty cycle, 30 s each, Amp10). Protein concentration was determined using a bicinchoninic acid (BCA) protein assay kit (Thermo Scientific), and the absorbance was read with a BioTek Cytation1 plate reader following manufacturer's instructions. For click reaction, a separate aliquot of ca. 50 μg of proteins from each sample was put in a 1.5 mL centrifuge tube and was mixed with freshly prepared Cy5-azide (2 mM in DMSO, 2.5 μL/sample,), $CuSO_4$ (150.9 mM in H_2O, 0.7 μL/sample), and then a mixture of TBTA (43 mM in 1:4 DMSO/*t*-BuOH, 0.23 μL/sample) and TCEP (272.6 mM in H_2O, 0.4 μL/sample). Each reaction mixture was made up to 50 μL final volume by adding DPBS and mixed by vortexing. The reaction was kept at rt for 1 h before being quenched with 50 μL of ice-cold MeOH. Cold DPBS (50 μL) was added to the mixture, followed by cold MeOH (150 μL), $CHCl_3$ (50 μL), and water (300 μL) (MeOH/$CHCl_3$/buffer in a final ratio of 4/1/7 v/v/v). The cloudy solution was thoroughly vortexed and then centrifuged (21,000*g*, 20 min, 4 °C) to separate the protein fraction from the aqueous and organic layers. The protein fraction was washed with cold MeOH (3×). The pelleted proteins were dried at rt, then resuspended in 100 μL of SDS lysis buffer, and sonicated in water bath until it was dissolved. Protein concentration in each sample was measured using a BCA protein assay kit. Proteins (5 μg/gel lane) were mixed with SDS loading buffer (4x stock), boiled at 95 °C, loaded in sodium dodecyl sulfate−polyacrylamide gel electrophoresis (SDS-PAGE) gel (containing 10% acrylamide), developed, and visualized by Coomassie blue staining or by the in-gel fluorescence on an Amersham Typhoon fluorescence scanner. The gel fluorescence and images were processed with the GE Typhoon Trio ImageQuant TL image analysis software.

MS-Based Analysis of Labeled Proteins

Cell lysis, tagging of the labeled proteins with biotin using biotin-azide instead of Cy5-azide for click reaction, and protein isolation from cell lysate followed the same protocols described above. The protein fractions were washed with MeOH, pelleted, and then resuspended in and incubated with a freshly prepared pre-equilibrated solution of streptavidin agarose resin in DPBS (300 μL) at rt for 2 h with end-to-end rotation. The streptavidin beads were separated by centrifugation (1500*g*, 2 min) and washed with 0.2% SDS in DPBS (3 × 2 mL) and H_2O (3 × 2 mL). The beads were finally applied to MS-based proteomics analysis.

MS Sample Preparation and Conditions

On-Bead Trypsin Digestion of Proteins. Protein-loaded beads obtained above were diluted with 50 mM ammonium bicarbonate. The samples were treated with 4 mM dithiothreitol (DTT) at 65 °C for 15 min and 10 mM chloroacetamide (CAA) at rt for 30 min in the dark. Then, the beads were treated with 500 ng trypsin at 37 °C overnight. Tryptic peptides were desalted with ZipTip by the manufacture's protocol (MilliporeSigma). The peptides were lyophilized at 160 mBar using a SpeedVac and resuspended in 0.1% formic acid (FA) for liquid chromatography−mass spectrometry (LC-MS) analysis. Two valid replicates for each genotype were prepared for proteomics analysis.

Liquid Chromatography−Tandem Mass Spectrometry (LC-MS/MS)-Based Proteomics Study. Proteomics data acquisition was achieved on an EASY-nLC 1200 System coupled with Orbitrap Fusion Mass Spectrometers (Thermo Fisher Scientific, Inc.). Samples were loaded to an Acclaim PepMap 100 C18 trapping column (75 μm i.d. × 2 cm, 3 μm, 100 Å) and separated on a PepMap C18 analytical column (75 μm i.d. × 25 cm, 2 μm, 100 Å). The flow rate was set at 250 nL/min with solvent A (0.1% FA in water) and solvent B (0.1% FA and 80% ACN in water) as the mobile phases. Separation was conducted using the following gradients: 2−35% of B over 0−70 min; 35−80% of B over 70−75 min; 80−98% of B over 75−76 min, and isocratic at 98% of B over 76−90 min. For MS data acquisition, the full MS1 scan (m/z 350−1800) was performed on the Orbitrap with a resolution of 120,000. The automatic gain control (AGC) target is 2e5 with 50 ms as the maximum injection time (MIT). Peptides bearing +2−6 charges were selected with an intensity threshold of 1e4. Dynamic exclusion of 30 s was used to prevent resampling the high abundance peptides, and the quadrupole isolation window was 1.3 Th. Fragmentation of the top 10 selected peptides by collision-induced dissociation (CID) was done at 35% of normalized collision energy. The MS2 spectra were acquired at an Ion Trap with AGC target as 1e4 and the maximum injection time as 35 ms.

Data Analysis. Proteome DiscovererTM (version 2.5, Thermo Scientific) was used to search the MS/MS spectra from the protein sample. The SEQUEST algorithm in the Proteome Discoverer was used to process raw data files. Spectra were searched using the UniProt homo sapiens protein database with the following parameters: 10 ppm mass tolerance for MS1 and 0.6 mass tolerance for MS2, two maximum missed tryptic cleavage sites, a fixed modification of carbamidomethylation (+57.021) on cysteine residues, and dynamic modifications of oxidation of methionine (+15.996). Search results were filtered at a 1% false discovery rate (FDR) and at least two unique peptides per protein for protein identification. Relative protein abundance in the samples was measured using label-free quantification, and proteins identified and quantified in all biological samples were used. No

https://doi.org/10.1021/acs.jproteome.2c00728
J. Proteome Res. 2023, 22, 919−930

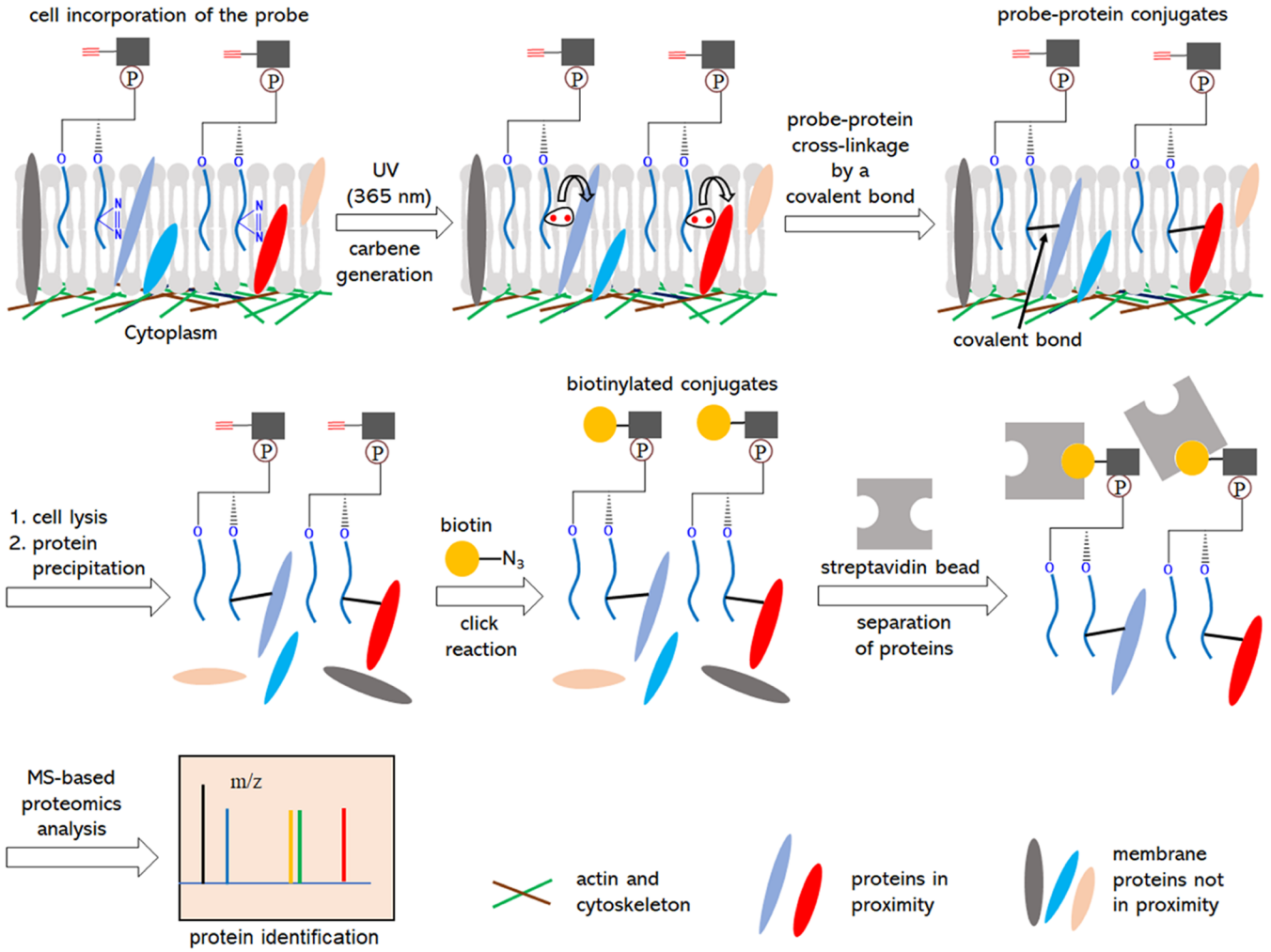

Figure 2. Schematic representation of the experimental design used to pull down GPI-interacting proteins in the cell membrane for proteomics analysis. Upon incubation with cells, synthetic probes **1** and **2** are incorporated into the cell membrane. UV irradiation of the probes on the cell generates a reactive carbene in the lipid chain of the probe, which can form a covalent bond with neighboring proteins. Click reaction between cross-linked proteins and azide-modified biotin labels the targets with biotin to facilitate their isolation using streptavidin-modified beads. The proteins attached to the bead are subjected to proteomic analysis according to conventional protocols.

imputation was performed. Peptides in samples were quantified as area under the chromatogram peak. FDR cutoffs for both peptide and protein identification were set as 1%.

Data Availability Statement

The datasets presented in this study can be found in online repositories. The names of the repositories and the accession number(s) are the following. The proteomics raw data and search results have been deposited to the ProteomeXchange Consortium via the PRIDE partner repository with the dataset identifier PXD0304719.

RESULTS AND DISCUSSION

Research Designs

To investigate GPI−cell membrane interactions and identify membrane proteins that bind with GPI anchors, we need a bifunctional probe, which can couple with GPI-interacting proteins and, in the meantime, link to an affinity tag to facilitate the isolation of labeled proteins. To this end, we designed and synthesized probe **1** (Figure 1),[23] which has several valuable features. First, it contains the highly conserved pseudodisaccharide motif, α-D-glucosaminyl-(1 → 6)-inositol, of the core structure found in all natural GPIs and the common diacyl phosphatidyl moiety. Thus, it is a general and representative GPI analogue. Second, probe **1** has a photoreactive diazirine group in the *O*-2-acyl group of its phosphatidyl moiety. Diazirines can be effectively activated by UV light at 365 nm to generate reactive carbenes, which can react with molecules in proximity to create a covalent bond.[27−29] This design will facilitate the cross-linkage of probe **1** and membrane proteins close to or interacting with its lipid moiety, thereby to label the proteins. The most common lipids found in natural GPIs are C16−C20 fatty acyl groups. Probe **1** contained a C18-stearic group with the diazirine group at the *C*-12-position that is located in the outer layer of the cell membrane—not too close to either the cell surface or the interface of the lipid bilayer. However, it is anticipated that the lipid structure and the diazirine group location in the lipid chain are likely to influence GPI organization and interaction with other molecules in the membrane and, hence, have an impact on the results. How these structural features would affect GPI anchor−membrane protein interactions is an interesting topic, which can be explored with probes that contain different lipids and/or have the diazirine group at

https://doi.org/10.1021/acs.jproteome.2c00728
J. Proteome Res. 2023, 22, 919−930

Scheme 1. Synthesis of 2 from Methyl α-D-Glucopyranoside 3

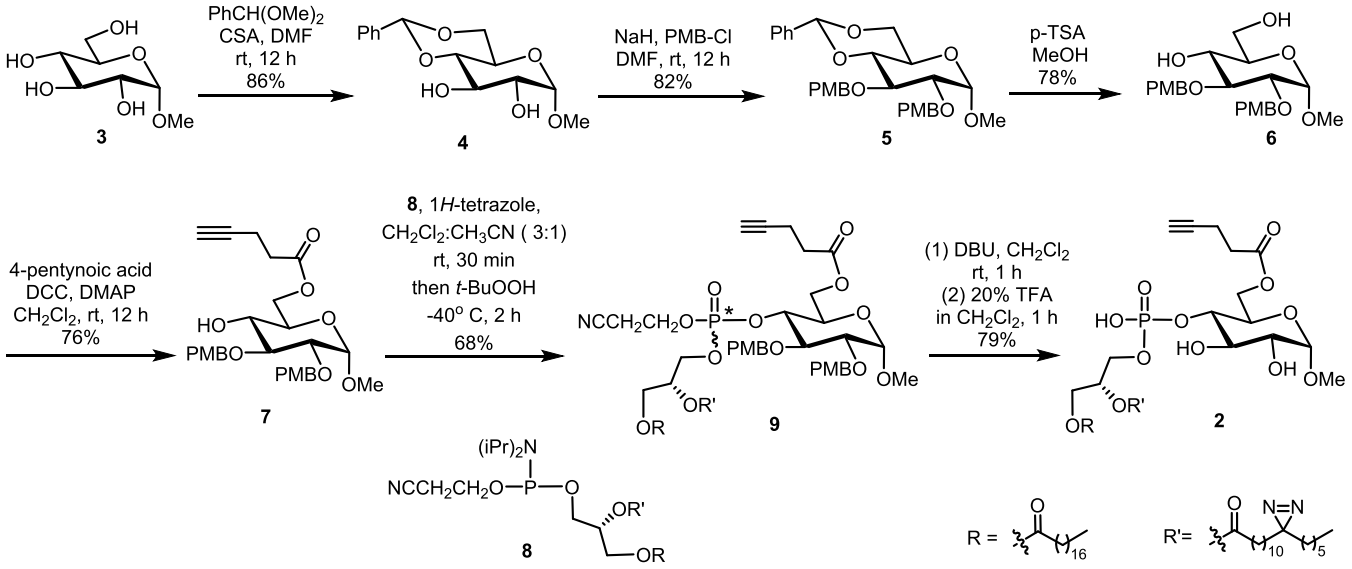

different positions. Third, probe **1** has an alkynyl group at the glucosamine 4′-*O*-position. It has been well established that alkynes can selectively react with azides under mild conditions[30−32] to enable the installment of an affinity tag to labeled proteins by a click reaction for their rapid isolation and proteomics analysis. In addition, the glucosamine 4′-*O*-position is where the GPI glycan is elongated for protein attachment in natural GPI-APs, thus an acyl group at this position blocks probe **1** from participating in GPI and GPI-AP biosynthesis, thereby to decrease the labeling of GPI-APs and reduce the background of proteomics study. Finally, the diazirine and the alkynoic groups are rather small, which are expected to have minimal impacts on probe **1** as a GPI analogue to interact with cell membrane proteins. In the meantime, we have designed and synthesized glycolipid **2** as a negative control, which has the same phosphatidyl moiety but a different glycan that does not possess the unique inositol residue of GPIs. Therefore, comparing the compositions of proteins pulled down by probes **1** and **2** may provide insights into the functional roles of inositol in the organization and recognition of GPI anchors on the cell surface.

Our experimental design for protein pull-down and proteomics analysis is delineated in Figure 2. It was anticipated that upon incubation with live cells, both probes **1** and **2** would be incorporated into the cell membrane, which has been demonstrated with synthetic lipids and glycolipids, as well as synthetic GPI and GPI-AP analogues.[21,33] This strategy has also been widely adopted to study live cells and cell membranes. In the meantime, we utilized the fluorescent labeling method to validate the incorporation of **1** and **2** into the cell membrane and guide the optimization of conditions. Next, the treated cells were subjected to UV irradiation to achieve the cross-coupling between the probe and GPI-interacting or adjacent membrane proteins, thereby to label these proteins. Photoaffinity labeling-based proteomics analysis has been demonstrated to be successful with various cells and systems.[34,35] Thereafter, the cells were lysed and treated with an azide-modified biotin derivative (biotin-azide) to install the affinity tag via Cu(I)-catalyzed alkyne-azide cycloaddition (CuAAC). This was followed by the isolation of cross-linked proteins using streptavidin-modified beads, and the pulled-down proteins were digested and applied to mass spectrometry (MS)-based proteomics analysis according to well-established protocols.

Synthesis of the Probes

The synthesis of probe **1** was described recently.[23] The synthesis of probe **2**, as outlined in Scheme 1, commenced with the conversion of commercially available methyl α-glucopyranoside **3** into **6** by a literature procedure.[36] Regioselective 4,6-*O*-benzylidenation of **3** upon reaction with benzaldehyde dimethyl acetal and camphorsulfonic acid (CSA) followed by protecting the remaining free hydroxyl groups in **4** with the *para*-methoxybenzyl (PMB) group afforded **5** in a 71% yield for two steps. PMB ethers can be selectively cleaved under mildly acidic conditions later. The 4,6-*O*-benzylidene group in **5** was then removed by trans-ketalization under the influence of *para*-toluenesulfonic acid (*p*-TSA) to provide **6**. Thereafter, **6** was acylated with 4-pentynoic acid using DCC as the condensation reagent in the presence of catalytic DMAP. The reaction was regioselective for the more reactive primary alcohol in **6** to generate **7**, which was confirmed by the significant down-field shift of the ^{1}H NMR signals for C6 protons. Compound **7** was smoothly phospholipidated with phosphoramidite **8** by an established two-step protocol to give **9** (68%) as a 1:1 diastereomeric mixture originated from the stereogenic phosphorus atom. Finally, **9** was treated with DBU and then with 20% TFA in CH_2Cl_2 to remove the cyanoethyl and PMB groups, respectively, to produce the synthetic target **2**, which was fully characterized with NMR and high-resolution MS data.

Cell Incorporation of Probes 1 and 2

To verify the effective incorporation of probes **1** and **2** into the plasma membrane by cells, we performed fluorescence labeling and imaging analysis of cells treated with **1** and **2**. In this experiment, Hela cells were incubated with **1** and **2** for 4 h in serum-free media, at which point cell incorporation of glycolipids should almost reach the peak according to a report.[37] This was followed by washing (to remove probes potentially remaining in the media) and UV (365 nm wavelength) irradiation for 15 min. Thereafter, the cells were incubated with azide-modified red fluorophore dye Cy5 (Cy5-

https://doi.org/10.1021/acs.jproteome.2c00728
J. Proteome Res. 2023, 22, 919−930

azide) under CuAAC conditions as mentioned above to attach Cy5 to the alkyne-functionalized probes on the cell. Finally, the cells were analyzed with a fluorescent microscope. It was shown that the cells treated with probes **1** and **2** were stained with Cy5-azide but not cells treated with PBS (Figure 3). The results clearly proved the labeling of cells by Cy5-azide, indicating the efficient incorporation of both probes by the cell.

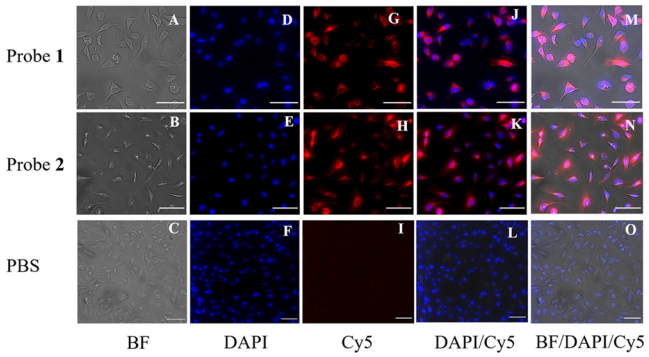

Figure 3. Bright-field (BF) (A−C) and DAPI (D−F) and Cy5 (G−I) fluorescent images of cells treated with probe **1**, probe **2**, or PBS (the negative control), and then with DAPI to stain DNA in the cell nucleus and Cy5-azide to stain alkyne-labeled probes. (J−L): overlays of DAPI and Cy5 images; (M−O): overlays of DAPI, Cy5, and BF images. The scale bars are 1 μm.

To further verify the above research design and the capability of these probes to label proteins in cells, we have also conducted SDS-PAGE analysis of cross-linked proteins. In this experiment, after UV irradiation of the probe-treated cells to allow for the cross-linkage of proteins with probes, the cells were lysed, and the lysates were incubated with biotin-azide in the presence of Cu(I) as a catalyst. Thereafter, the cell lysates containing normalized quantities of proteins were applied to SDS-PAGE. The developed gels were treated with streptavidin-Cy5 to label tagged proteins and analyzed with a fluorescence imager. The SDS-PAGE results (as shown in Figure S1, Supporting Information) clearly indicated that many proteins were labeled and pulled down by both probes **1** and **2**, in contrast to the negative control, suggesting the feasibility of investigating GPI-interacting cell membrane proteins by the designed probes and experimental protocols.

Analysis of GPI-Interacting Membrane Proteins Using Live Cells

These studies were performed according to the procedure outlined in Figure 2, using the conditions established by SDS-PAGE study. Here, the Hela cell line was selected because of its easy access and convenient proteome information, which would facilitate proteomics analysis.[38] Briefly, after incubation with the probes and UV irradiation, cells were lysed, and the cell lysates were treated with an azide-modified biotin and Cu(I). The methanol-chloroform protein precipitation method was then used to isolate proteins and, in the meantime, to remove excessive biotin-azide, lipids, and other biomolecules. The protein fraction was dissolved in SDS buffer and incubated with streptavidin beads. The loaded beads were isolated, washed, and finally subjected to MS-based proteomics analysis according to conventional protocols. Each experiment was duplicated to verify the results.

Proteomics analysis revealed ∼1500 and ∼1900 significant proteins pulled down by probe **1** and probe **2** (control), respectively. Among them, ∼1400 proteins were observed with both probes (Figure S2, Supporting Information). The volcano plot of various proteins pulled down by probe **1**, with proteins pulled down by the control probe **2** as references, is depicted in Figure 4A. It reveals 94 unique proteins that were observed with probe **1** but not with probe **2** (Table S1, Supporting Information) and these proteins had different abundancies as reflected by the $\log_2$ FC (FC: fold of changes). These proteins are supposed to be specifically associated with the $GlcNH_2$-Ino epitope of probe **1**. Among the 94 unique proteins, 58 were

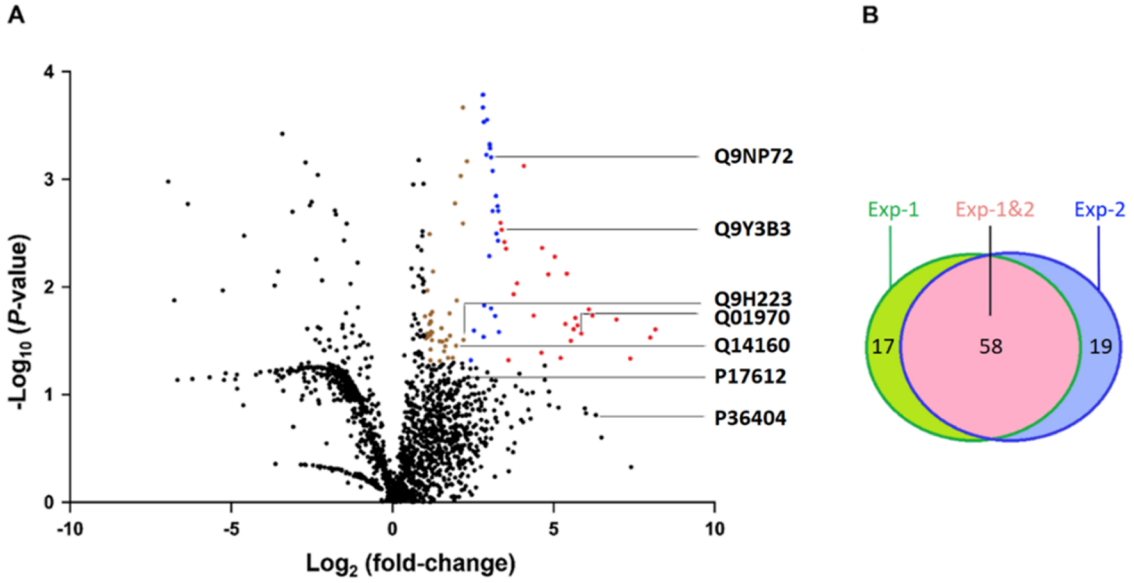

Figure 4. Volcano plot showing the distribution of all proteins pulled down by probe **1** presented in $\log_2$ FC (fold of change) and $\log_{10} P$, using proteins pulled down by probe **2** as controls (A). Color dots indicate statistically significant ($P < 0.05$) proteins that have an enrichment of ≥10-fold in red, ≥5-fold in blue, and ≥2-fold in brown. The labeled proteins are examples that are related to GPI-APs as reported in the literature. Schematic representation of the unique proteins pulled down by probe **1** observed in experiment 1 (green circle) and experiment 2 (blue circle), respectively, as well as those observed in both experiments (pink area) (B).

https://doi.org/10.1021/acs.jproteome.2c00728
J. Proteome Res. 2023, 22, 919−930

Table 1. Unique Proteins Pulled Down by Probe 1 That Are Potentially Related to GPI-APs

proteins	UniProt ID	literature reported functions and association with GPI-APs
PKAC	P17612	a cAMP-dependent protein kinase subunit. Cleavage of GPI-APs and endocytosis of different GPI-APs are regulated by PKAC class of proteins.[40,41,53−58]
SCRIB	Q14160	a protein at the cell−cell junction to regulate cell−cell adhesions in different epithelial cells. SCRIB controls CDC42 protein, which is an important factor in the recycling process of GPI-APs.[44−46,59]
YES1	P07947	a nonreceptor tyrosine kinase communicating signals generated from receptor tyrosine kinase to cytoplasm.[47]
RAB18	Q9NP72	a cell membrane protein, especially in lipid raft microdomains, that helps to localize different proteins required for raft formation.[60]
AP2S1	P53680	AP2 protein plays a role in clathrin-mediated endocytosis of plasma membrane proteomes.[61]
BAG6	P46379	one of the proteins that regulate quality control of proteins, thus playing an essential role in targeting transmembrane domains either to ER or degradation. BAG6 strongly favors long linear hydrophobic sequences such as ER targeting signals and GPI-anchoring signals.[48−50,62,63]
EHD4	Q9H223	EH domain-containing protein 4: a membrane-bound protein that mainly presents in early endosome membrane. EHD4 plays a role in membrane organization, tubulin formation, and endosomal transport. This protein is believed to regulate cell signaling of GPI-APs, but the mechanism is not clear.[51,61,64−67]
COPG2	Q9UBF2	protein export from ER exit sites to Golgi occurs, where COPG2 is an essential protein subunit.[52]
SMARCD1	Q96GM5	a cancer stem cell regulatory protein, which may be indirectly associated with Crypto1, a GPI-AP present in breast cancer stem cells.[68]
ARL2	P36404	a GTP binding protein that regulates the formation of microtubule. It plays a role in the exocytosis of GPI-APs.[69]
TMED7	Q9Y3B3	a protein present in ER membrane. Sorting of GPI-APs into ER exit sites is controlled by P24 protein complex, where TMED7 plays a significant role.[70,71]
Q01970	PLCB3	1-phosphatidylinositol 4,5-bisphosphate phosphodiesterase β-3: an enzyme involved in the production of secondary messenger molecules such as inositol-1,4,5-triphosphate (IP3) and diacylglycerol (DAG).[72,73]

observed in both experiments, and the other 17 and 19 proteins were identified in one of the duplicate experiments, respectively (Figure 4B). In addition, we have also identified 18 statistically significantly ($P \leq 0.05$) enriched (an enrichment of ≥5-fold) proteins with probe **1** (Table S2, Supporting Information) (Table S2, Supporting Information) compared to that of probe **2**. Overall, these results suggested that many proteins cross-linked to **1** but not or barely to **2**, which have the same lipid but different glycans.

The identities of all 94 unique proteins pulled down by probe **1**, as well as their locations and potential biological functions, were examined in detail and are listed in Table S2 in the Supporting Information. Clearly, most proteins are associated with membranes, either plasma membrane, intracellular organelle, or compartment membranes, suggesting the capability of probe **1** to target membranes. As expected, neither **1** nor **2** was specific for the plasma membrane because besides incorporation in the plasma membrane, glycolipids can also enter cells through endocytosis to be incorporated in intracellular membranes.[39] Shortening the incubation time of cells with the probe may help reduce intracellular labeling, which will be explored in the future. Nevertheless, this does not affect the value of **1** as a probe to study GPI−cell membrane interactions. Conversely, this may broaden the application scope of the probe. For example, most intracellular proteins pulled down by **1** are located in the ER and Golgi apparatus, where GPIs and GPI-APs are biosynthesized and transported. Therefore, probe **1** and its analogues may also be used to study GPI-AP metabolism and trafficking.

More importantly, several of the proteins pulled down by probe **1** (Tables 1 and S3 in the Supporting Information) are anticipated as being related to GPI-APs, including their trafficking and signaling. For example, protein kinase-A catalytic subunit (PKAC) is a cyclic adenosine monophosphate (cAMP)-dependent protein kinase subunit localized in the plasma membrane, which is involved in several signaling pathways. GPI-based domains provide an integration site for signaling involved in CD59 (a GPI-AP) endocytosis,[40] whereas cleavage of GPI-APs by phospholipase D can activate protein kinase Cα (PKCα),[41] and G protein-coupled receptors (GPCRs) also relay the binding signals in a cAMP-dependent manner.[42] Scribble protein (SCRIB) is engaged in cell adhesion.[43,44] Although there is no report directly associating SCRIB with GPI-APs yet, we anticipate that they are also corrrelated, based on the fact that SCRIB regulates the activity and localization of CDC42 protein,[45,46] a major component in GPI-AP endocytosis. YES1, which is a nonreceptor tyrosine kinase (NRTK) at the interface of cytoplasm and plasma membrane,[47] relays binding signals generated from tyrosine kinase receptor (RTK) or other extracellular receptors, a process that is associated with GPI-APs. B-cell lymphoma 2 (BCL2)-associated athanogene cochaperone 6 (Bag6) is a protein present in the extracellular region of cell membrane, which has a broad specificity to bind with hydrophobic regions, such as the sequences of GPI-anchoring signals, in mislocalized membrane proteins to prevent their aggregation,[48,49] thus playing an important role in quality control of GPI-APs and other proteins.[50] Eps15 homology (EH) domain-containing protein 4 (EHD4) is a member of the EHD protein family that interacts with the cholesterol-rich region of the membrane and helps GPI-AP vesiculation.[51] Coat protein complex I (COPI) subunit γ 2 (COPG2) protein is known to play a role in protein transport from the ER to Golgi by forming vesicles at the ER exit site to help ER export of GPI-APs.[52]

To better understand the profiles of proteins pulled down by probe **1**, we conducted additional bioinformatics analysis. Ontology studies of the genes with respect to biological processes showed that the unique proteins with high enrichments are related to posttranslational modifications (Figure 5), which is expected since GPI-APs and most membrane proteins are post-translationally modified and signaling events often engage translational modifications of proteins. Our studies also revealed that some proteins, especially those enriched but nonunique proteins (listed in Table S2, Supporting Information), are related to cell endocytosis, rRNA processing, and transcription, which is likely because of the probe incorporation into intracellular membranes. Ontology studies of the genes with respect to biological functions suggested that many of the unique proteins pulled down by probe **1** have a strong binding affinity toward proteins, guanosine triphosphate (GTP), and guanosine diphosphate (GDP), which is also expected because

https://doi.org/10.1021/acs.jproteome.2c00728
J. Proteome Res. 2023, 22, 919−930

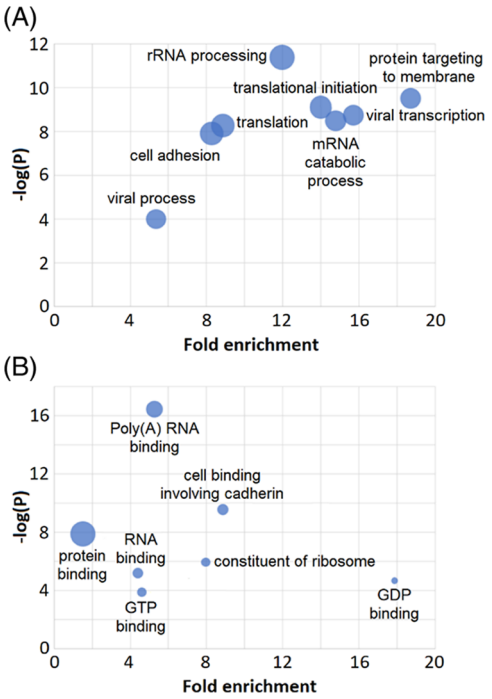

Figure 5. Gene ontology analysis of the 94 unique proteins pulled down by probe **1** with respect to biological processes (A) and biological functions (B). The *X* axis shows the folds of enrichment of proteins pulled down by probe **1**, compared to proteins pulled down by probe **2**, and the *Y* axis shows the statistical significance. The bubble sizes are relative and proportional to the number of proteins in the dataset with similar or related activities.

GTPases involved in signaling events tend to present at the interface of plasma membrane and cytosol. Some of the pulled-down proteins are associated with RNA binding, which may be due to the labeling of intracellular membranes.

CONCLUSIONS

In this work, we have demonstrated the design and application of a photoaffinity approach for the investigation of membrane proteins (or proteome) associated with GPI-APs in Hela cells. It represents the first report on this topic. The designed probe **1** has small diazirine and alkyne labels attached to the conserved core disaccharide of GPI anchors to assure its close mimic to the natural structure. We have proved by different methods that probe **1** and its analogue **2**, which serves as a negative control, were efficiently incorporated in the cell membrane. More importantly, comparing the proteins pulled down by probes **1** and **2** revealed a series of unique and highly enriched proteins associated with **1**. In addition, the duplicated experiments produced similar results, suggesting the reliability and reproducibility of the approach.

Bioinformatics analysis of the unique and enriched proteins pulled down by probe **1** disclosed that they are mainly membrane proteins. Although the functions for the majority of these proteins are not described in the literature yet, the functions of the reported proteins are primarily related to signaling or similar activities engaging GTP, GDP, and various protein kinases. Moreover, many of the identified proteins are GPI-AP-related (Table 1). For example, EHD4, BAG6, SCRIB, and YES1 proteins are involved in the metabolism, trafficking, and signaling of GPI-APs. These results indicate that probe **1** has indeed targeted the plasma membrane, as well as membranes in the cell, and hence should be a useful tool for the investigation of GPI anchor interactions with the plasma membrane. Accordingly, the proteomics dataset produced herewith should be valuable for further data mining to discover novel GPI-interacting proteins, as well as other proteins involved in GPI metabolism, trafficking, etc. The next stage of this work is to explore the functions of the unique proteins pulled down by **1** using gene-engineering technologies to overexpress or downregulate specific proteins and analyzing the interactions of these proteins with GPI anchors and GPI-APs. In this regard, the relationships of the proteins with the signaling pathways of GPI-APs should be particularly interesting.

This work has validated the proposed photoaffinity approach for the study of GPI interactions with the cell membrane, and the approach should be generally applicable to other studies using the same or different probes. However, probe **1** consists of only the pseudodisaccharide moiety of the core structure of all natural GPI anchors and a common lipid form. Thus, probe **1** was expected to be general, to result in the cross-linkage and characterization of a broad spectrum of proteins. On the other hand, using probes that are equipped with the same functionalities but contain the GPI anchor of specific GPI-APs that are unique in terms of both the lipid and the glycan, we anticipate the identification of specific membrane proteins for individual GPI-APs. Furthermore, comparing the results obtained with probe **1** to those obtained with other GPI probes carrying different glycans and lipids will provide additional information concerning the biological functions of GPI anchors, as well as the influences of their glycan and lipid structures on the GPI interactions with the cell membrane. Consequently, another direction of this project is to synthesize more photoaffinity GPI probes and apply them to the exploration of GPI-binding membrane proteins by the same strategy and protocols, which is currently pursued in our laboratory.

In addition, although the HeLa cell line was selected as the model in this research due to the reasons mentioned above, probe **1** should be widely applicable to other cell lines. The results of HeLa cells are likely to be different from those of normal cells or other cancer cell lines. Studies and comparisons of GPI-interacting membrane proteins derived from different cells using the same probe and protocols will help discover novel biomarkers and related pathways and provide useful insights into the functional mechanisms of GPI-APs and their relationships with human diseases. This represents another important topic in GPI-AP research.

ASSOCIATED CONTENT

Supporting Information

The Supporting Information is available free of charge at https://pubs.acs.org/doi/10.1021/acs.jproteome.2c00728.

SDS-PAGE results of proteins obtained from Hela cells treated with probes **1** and **2** and the negative control; total numbers of proteins pulled down by probes **1** and **2**; unique proteins pulled down by probe **1**; statistically significantly enriched proteins ($P \leq 0.05$, ≥5-fold of enhancement) pulled down by probe **1**; unique proteins pulled down by **1**, which are reported in the literature as being related to GPI-APs; and NMR and HR MS spectra of probe **2** and its synthetic intermediates (PDF)

https://doi.org/10.1021/acs.jproteome.2c00728
J. Proteome Res. 2023, 22, 919−930

AUTHOR INFORMATION

Corresponding Author

Zhongwu Guo − *Department of Chemistry, University of Florida, Gainesville, Florida 32611, United States;* orcid.org/0000-0001-5302-6456; Email: zguo@che.ufl.edu

Authors

Sayan Kundu − *Department of Chemistry, University of Florida, Gainesville, Florida 32611, United States*

Chuwei Lin − *Department of Biology, Genetics Institute, University of Florida, Gainesville, Florida 32611, United States*

Mohit Jaiswal − *Department of Chemistry, University of Florida, Gainesville, Florida 32611, United States*

Venkanna Babu Mullapudi − *Department of Chemistry, University of Florida, Gainesville, Florida 32611, United States*

Kendall C. Craig − *Department of Chemistry, University of Florida, Gainesville, Florida 32611, United States*

Sixue Chen − *Department of Biology, Genetics Institute, University of Florida, Gainesville, Florida 32611, United States;* Present Address: Department of Biology, University of Mississippi, Oxford, Mississippi 38677, United States; orcid.org/0000-0002-6690-7612

Complete contact information is available at: https://pubs.acs.org/10.1021/acs.jproteome.2c00728

Author Contributions

‖S.K., C.L., and M.J. contributed equally to this work. The manuscript was written through contributions of all authors. All authors have given approval to the final version of the manuscript.

Notes

The authors declare no competing financial interest.

ACKNOWLEDGMENTS

This work was supported by an NIH/NIGMS Grant (1R35 GM131686). Z.G. is also grateful to Steven and Rebecca Scott for endowing our research.

REFERENCES

(1) Cho, W.; Stahelin, R. V. Membrane-protein interactions in cell signaling and membrane trafficking. *Annu. Rev. Biophys. Biomol. Struct.* **2005**, *34*, 119−151.

(2) Brown, D.; Waneck, G. L. Glycosylphosphatidylinositol-anchored membrane proteins. *J. Am. Soc. Nephrol.* **1992**, *3*, 895−906.

(3) Kinoshita, T.; Fujita, M. Biosynthesis of GPI-anchored proteins: special emphasis on GPI lipid remodeling. *J. Lipid Res.* **2016**, *57*, 6−24.

(4) Englund, P. T. The structure and biosynthesis of glycosyl phosphatidylinositol protein anchors. *Annu. Rev. Biochem.* **1993**, *62*, 121−138.

(5) Kinoshita, T. Biosynthesis and biology of mammalian GPI-anchored proteins. *Open Biol.* **2020**, *10*, No. 190290.

(6) Ferguson, M. A. J.; Williams, A. F. Cell-surface anchoring of proteins via glycosylphosphatidylinositol structure. *Annu. Rev. Biochem.* **1988**, *57*, 285−320.

(7) Hwa, K.-y. Glycosyl phosphatidylinositol-linked glycoconjugates: structure, biosynthesis and function. *Adv. Exp. Med. Biol.* **2001**, *491*, 207−214.

(8) Paulick, M. G.; Bertozzi, C. R. The glycosylphosphatidylinositol anchor: A complex membrane-anchoring structure for proteins. *Biochemistry* **2008**, *47*, 6991−7000.

(9) Trotter, J.; Klein, C.; Kramer, E. GPI-anchored proteins and glycosphingolipid-rich rafts: Platforms for adhesion and signaling. *Neuroscientist* **2000**, *6*, 271−284.

(10) Robinson, P. J. Signal transduction by GPI-anchored membrane proteins. *Cell Biol. Int. Rep.* **1991**, *15*, 761−767.

(11) Um, J. W.; Ko, J. Neural Glycosylphosphatidylinositol-Anchored Proteins in Synaptic Specification. *Trends Cell Biol.* **2017**, *27*, 931−945.

(12) Deckert, M.; Ticchioni, M.; Mari, B.; Mary, D.; Bernard, A. The glycosylphosphatidylinositol-anchored CD59 protein stimulates both T cell receptor zeta/ZAP-70-dependent and -independent signaling pathways in T cells. *Eur. J. Immunol.* **1995**, *25*, 1815−1822.

(13) Li, C.; Yeh, F. L.; Cheung, A. Y.; Duan, Q.; Kita, D.; Liu, M. C.; Maman, J.; Luu, E. J.; Wu, B. W.; Gates, L.; Jalal, M.; Kwong, A.; Carpenter, H.; Wu, H. M. Glycosylphosphatidylinositol-anchored proteins as chaperones and co-receptors for FERONIA receptor kinase signaling in Arabidopsis. *eLife* **2015**, *4*, No. e06587.

(14) Sharom, F. J.; Radeva, G. GPI-anchored protein cleavage in the regulation of transmembrane signals. *Subcell. Biochem.* **2004**, *37*, 285−315.

(15) Balatskaya, M. N.; Sharonov, G. V.; Baglay, A. I.; Rubtsov, Y. P.; Tkachuk, V. A. Different spatiotemporal organization of GPI-anchored T-cadherin in response to low-density lipoprotein and adiponectin. *Biochim. Biophys. Acta, Gen. Subj.* **2019**, *1863*, No. 129414.

(16) Sahu, P. K.; Tomar, R. S. The natural anticancer agent cantharidin alters GPI-anchored protein sorting by targeting Cdc1-mediated remodeling in endoplasmic reticulum. *J. Biol. Chem.* **2019**, *294*, 3837−3852.

(17) Tiveron, M. C.; Nosten-Bertrand, M.; Jani, H.; Garnett, D.; Hirst, E. M.; Grosveld, F.; Morris, R. J. The mode of anchorage to the cell surface determines both the function and the membrane location of Thy-1 glycoprotein. *J. Cell Sci.* **1994**, *107*, 1783−1796.

(18) Stefanová, I.; Horejsí, V.; Ansotegui, I. J.; Knapp, W.; Stockinger, H. GPI-anchored cell-surface molecules complexed to protein tyrosine kinases. *Science* **1991**, *254*, 1016−1019.

(19) Bate, C.; Williams, A. Monoacylated cellular prion protein modifies cell membranes, inhibits cell signaling, and reduces prion formation. *J. Biol. Chem.* **2011**, *286*, 8752−8758.

(20) Nicholson, T. B.; Stanners, C. P. Specific inhibition of GPI-anchored protein function by homing and self-association of specific GPI anchors. *J. Cell Biol.* **2006**, *175*, 647−659.

(21) Raghupathy, R.; Anilkumar, A. A.; Polley, A.; Singh, P. P.; Yadav, M.; Johnson, C.; Suryawanshi, S.; Saikam, V.; Sawant, S. D.; Panda, A.; Guo, Z.; Vishwakarma, R. A.; Rao, M.; Mayor, S. Transbilayer lipid Interactions mediate nanoclustering of lipid-anchored proteins. *Cell* **2015**, *161*, 581−594.

(22) Horejsí, V.; Cebecauer, M.; Cerný, J.; Brdicka, T.; Angelisová, P.; Drbal, K. Signal transduction in leucocytes via GPI-anchored proteins: an experimental artefact or an aspect of immunoreceptor function? *Immunol. Lett.* **1998**, *63*, 63−73.

(23) Mullapudi, V. B.; Craig, K. C.; Guo, Z. Design and Synthesis of a Doubly Functionalized Core Structure of a Glycosylphosphatidylinositol Anchor Containing Photoreactive and Clickable Functional Groups. *J. Org. Chem.* **2022**, *87*, 9419−9425.

(24) Neef, A. B.; Schultz, C. Selective fluorescence labeling of lipids in living cells. *Angew. Chem., Int. Ed.* **2009**, *48*, 1498−5100.

(25) Parker, C. G.; Galmozzi, A.; Wang, Y.; Correia, B. E.; Sasaki, K.; Joslyn, C. M.; Kim, A. S.; Cavallaro, C. L.; Lawrence, R. M.; Johnson, S. R.; Narvaiza, I.; Saez, E.; Cravatt, B. F. Ligand and Target Discovery by Fragment-Based Screening in Human Cells. *Cell* **2017**, *168*, 527−541.

(26) Niphakis, M. J.; Lum, K. M.; Cognetta, A. B.; Correia, B. E.; Ichu, T. A.; Olucha, J.; Brown, S. J.; Kundu, S.; Piscitelli, F.; Rosen, H.; Cravatt, B. F. A Global Map of Lipid-Binding Proteins and Their Ligandability in Cells. *Cell* **2015**, *161*, 1668−1680.

(27) Dubinsky, L.; Krom, B. P.; Meijler, M. M. Diazirine based photoaffinity labeling. *Bioorg. Med. Chem.* **2012**, *20*, 554−570.
(28) Moss, R. A. Diazirines: Carbene precursors par excellence. *Acc. Chem. Res.* **2006**, *39*, 267−272.
(29) Das, J. Aliphatic diazirines as photoaffinity probes for proteins: Recent development. *Chem. Rev.* **2011**, *111*, 4405−4417.
(30) Kolb, H. C.; Finn, M. G.; Sharpless, K. B. Click chemistry: Diverse chemical function from a few good reactions. *Angew. Chem., Int. Ed.* **2001**, *40*, 2004−2021.
(31) Takayama, Y.; Kusamori, K.; Nishikawa, M. Click chemistry as a tool for cell engineering and drug delivery. *Molecules* **2019**, *24*, No. 172.
(32) Dehnert, K. W.; Baskin, J. M.; Laughlin, S. T.; Beahm, B. J.; Naidu, N. N.; Amacher, S. L.; Bertozzi, C. R. Imaging the sialome during zebrafish development with copper-free click chemistry. *ChemBioChem* **2012**, *13*, 353−357.
(33) Paulick, M. G.; Wise, A. R.; Forstner, M. B.; Groves, J. T.; Bertozzi, C. R. Synthetic analogues of glycosylphosphatidylinositol-anchored proteins and their behavior in supported lipid bilayers. *J. Am. Chem. Soc.* **2007**, *129*, 11543−11550.
(34) Xia, Y.; Peng, L. Photoactivatable lipid probes for studying biomembranes by photoaffinity labeling. *Chem. Rev.* **2013**, *113*, 7880−7929.
(35) Wright, M. H.; Sieber, S. A. Chemical proteomics approaches for identifying the cellular targets of natural products. *Nat. Prod. Rep.* **2016**, *33*, 681−708.
(36) Yamamoto, K.; Noguchi, S.; Takada, N.; Miyairi, K.; Hashimoto, M. Synthesis of a trigalacturonic acid analogue mimicking the expected transition state in the glycosidases. *Carbohydr. Res.* **2010**, *345*, 572−585.
(37) Paulick, M. G.; Forstner, M. B.; Groves, J. T.; Bertozzi, C. R. A chemical approach to unraveling the biological function of the glycosylphosphatidylinositol anchor. *Proc. Natl. Acad. Sci. U.S.A.* **2007**, *104*, 20332−20337.
(38) Nagaraj, N.; Wisniewski, J. R.; Geiger, T.; Cox, J.; Kircher, M.; Kelso, J.; Pääbo, S.; Mann, M. Deep proteome and transcriptome mapping of a human cancer cell line. *Mol. Syst. Biol.* **2011**, *7*, No. 548.
(39) Johannes, L.; Wunder, C.; Shafaq-Zadah, M. Glycolipids and lectins in endocytic uptake processes. *J. Mol. Biol.* **2016**, *428*, 4792−4818.
(40) Deckert, M.; Ticchioni, M.; Bernard, A. Endocytosis of GPI-anchored proteins in human lymphocytes: role of glycolipid-based domains, actin cytoskeleton, and protein kinases. *J. Cell Biol.* **1996**, *133*, 791−799.
(41) Tsujioka, H.; Takami, N.; Misumi, Y.; Ikehara, Y. Intracellular cleavage of glycosylphosphatidylinositol by phospholipase D induces activation of protein kinase Calpha. *Biochem. J.* **1999**, *342*, 449−455.
(42) Calebiro, D.; Nikolaev, V. O.; Gagliani, M. C.; de Filippis, T.; Dees, C.; Tacchetti, C.; Persani, L.; Lohse, M. J. Persistent cAMP-signals triggered by internalized G-protein-coupled receptors. *PLoS Biol.* **2009**, *7*, No. e1000172.
(43) Nagasaka, K.; Nakagawa, S.; Yano, T.; Takizawa, S.; Matsumoto, Y.; Tsuruga, T.; Nakagawa, K.; Minaguchi, T.; Oda, K.; Hiraike-Wada, O.; Ooishi, H.; Yasugi, T.; Taketani, Y. Human homolog of Drosophila tumor suppressor Scribble negatively regulates cell-cycle progression from G1 to S phase by localizing at the basolateral membrane in epithelial cells. *Cancer Sci.* **2006**, *97*, 1217−1225.
(44) Zhan, L.; Rosenberg, A.; Bergami, K. C.; Yu, M.; Xuan, Z.; Jaffe, A. B.; Allred, C.; Muthuswamy, S. K. Deregulation of scribble promotes mammary tumorigenesis and reveals a role for cell polarity in carcinoma. *Cell* **2008**, *135*, 865−878.
(45) Osmani, N.; Vitale, N.; Borg, J. P.; Etienne-Manneville, S. Scrib controls Cdc42 localization and activity to promote cell polarization during astrocyte migration. *Curr. Biol.* **2006**, *16*, 2395−2405.
(46) Dow, L. E.; Elsum, I. A.; King, C. L.; Kinross, K. M.; Richardson, H. E.; Humbert, P. O. Loss of human Scribble cooperates with H-Ras to promote cell invasion through deregulation of MAPK signalling. *Oncogene* **2008**, *27*, 5988−6001.
(47) Uddin, M. E.; Garrison, D. A.; Kim, K.; Jin, Y.; Eisenmann, E. D.; Huang, K. M.; Gibson, A. A.; Hu, Z.; Sparreboom, A.; Hu, S. Influence of YES1 Kinase and Tyrosine Phosphorylation on the Activity of OCT1. *Front. Pharmacol.* **2021**, *12*, No. 644342.
(48) Mock, J. Y.; Chartron, J. W.; Zaslaver, M.; Xu, Y.; Ye, Y.; Clemons, W. M., Jr. Bag6 complex contains a minimal tail-anchor-targeting module and a mock BAG domain. *Proc. Natl. Acad. Sci. U.S.A.* **2015**, *112*, 106−111.
(49) Hegde, R. S.; Zavodszky, E. Recognition and Degradation of Mislocalized Proteins in Health and Disease. *Cold Spring Harbor Perspect. Biol.* **2019**, *11*, No. a033902.
(50) Benarroch, R.; Austin, J. M.; Ahmed, F.; Isaacson, R. L. The roles of cytosolic quality control proteins, SGTA and the BAG6 complex, in disease. *Adv. Protein Chem. Struct. Biol.* **2019**, *114*, 265−313.
(51) Cai, B.; Caplan, S.; Naslavsky, N. cPLA2α and EHD1 interact and regulate the vesiculation of cholesterol-rich, GPI-anchored, protein-containing endosomes. *Mol. Biol. Cell* **2012**, *23*, 1874−1888.
(52) Lopez, S.; Rodriguez-Gallardo, S.; Sabido-Bozo, S.; Muñiz, M. Endoplasmic Reticulum Export of GPI-Anchored Proteins. *Int. J. Mol. Sci.* **2019**, *20*, No. 3506.
(53) Guan, H.; Hou, S.; Ricciardi, R. P. DNA binding of repressor nuclear factor-kappaB p50/p50 depends on phosphorylation of Ser337 by the protein kinase A catalytic subunit. *J. Biol. Chem.* **2005**, *280*, 9957−9962.
(54) D'Souza, T.; Agarwal, R.; Morin, P. J. Phosphorylation of claudin-3 at threonine 192 by cAMP-dependent protein kinase regulates tight junction barrier function in ovarian cancer cells. *J. Biol. Chem.* **2005**, *280*, 26233−26240.
(55) Pearson, G. W.; Earnest, S.; Cobb, M. H. Cyclic AMP selectively uncouples mitogen-activated protein kinase cascades from activating signals. *Mol. Cell Biol.* **2006**, *26*, 3039−3047.
(56) Bullen, J. W.; Tchernyshyov, I.; Holewinski, R. J.; DeVine, L.; Wu, F.; Venkatraman, V.; Kass, D. L.; Cole, R. N.; Van Eyk, J.; Semenza, G. L. Protein kinase A-dependent phosphorylation stimulates the transcriptional activity of hypoxia-inducible factor 1. *Sci. Signal.* **2016**, *9*, No. ra56.
(57) Lee, J. W.; Lee, J.; Moon, E. Y. HeLa human cervical cancer cell migration is inhibited by treatment with dibutyryl-cAMP. *Anticancer Res.* **2014**, *34*, 3447−3455.
(58) Koinuma, S.; Takeuchi, K.; Wada, N.; Nakamura, T. cAMP-induced activation of protein kinase A and p190B RhoGAP mediates down-regulation of TC10 activity at the plasma membrane and neurite outgrowth. *Genes Cells* **2017**, *22*, 953−967.
(59) Qin, Y.; Capaldo, C.; Gumbiner, B. M.; Macara, I. G. The mammalian Scribble polarity protein regulates epithelial cell adhesion and migration through E-cadherin. *J. Cell Biol.* **2005**, *171*, 1061−1071.
(60) Dejgaard, S. Y.; Presley, J. F. Rab18: new insights into the function of an essential protein. *Cell. Mol. Life Sci.* **2019**, *76*, 1935−1945.
(61) Tobys, D.; Kowalski, L. M.; Cziudaj, E.; Müller, S.; Zentis, P.; Pach, E.; Zigrino, P.; Blaeske, T.; Höning, S. Inhibition of clathrin-mediated endocytosis by knockdown of AP-2 leads to alterations in the plasma membrane proteome. *Traffic* **2021**, *22*, 6−22.
(62) Kawahara, H.; Minami, R.; Yokota, N. BAG6/BAT3: emerging roles in quality control for nascent polypeptides. *J. Biochem.* **2013**, *153*, 147−160.
(63) Wang, Q.; Liu, Y.; Soetandyo, N.; Baek, K.; Hegde, R.; Ye, Y. A ubiquitin ligase-associated chaperone holdase maintains polypeptides in soluble states for proteasome degradation. *Mol. Cell* **2011**, *42*, 758−770.
(64) George, M.; Ying, G.; Rainey, M. A.; Solomon, A.; Parikh, P. T.; Gao, Q.; Band, V.; Band, H. Shared as well as distinct roles of EHD proteins revealed by biochemical and functional comparisons in mammalian cells and C. elegans. *BMC Cell Biol.* **2007**, *8*, No. 3.
(65) Kuo, H. J.; Tran, N. T.; Clary, S. A.; Morris, N. P.; Glanville, R. W. Characterization of EHD4, an EH domain-containing protein expressed in the extracellular matrix. *J. Biol. Chem.* **2001**, *276*, 43103−43110.

https://doi.org/10.1021/acs.jproteome.2c00728
J. Proteome Res. 2023, 22, 919−930

(66) Daumke, O.; Lundmark, R.; Vallis, Y.; Martens, S.; Butler, P. J.; McMahon, H. T. Architectural and mechanistic insights into an EHD ATPase involved in membrane remodelling. *Nature* **2007**, *449*, 923−927.
(67) Jović, M.; Kieken, F.; Naslavsky, N.; Sorgen, P. L.; Caplan, S. Eps15 homology domain 1-associated tubules contain phosphatidylinositol-4-phosphate and phosphatidylinositol-(4,5)-bisphosphate and are required for efficient recycling. *Mol. Biol. Cell* **2009**, *20*, 2731−2743.
(68) Donaldson, J. G.; Jackson, C. L. ARF family G proteins and their regulators: roles in membrane transport, development and disease. *Nat. Rev. Mol. Cell Biol.* **2011**, *12*, 362−375.
(69) Price, H. P.; Panethymitaki, C.; Goulding, D.; Smith, D. F. Functional analysis of TbARL1, an N-myristoylated Golgi protein essential for viability in bloodstream trypanosomes. *J. Cell Sci.* **2005**, *118*, 831−841.
(70) Liaunardy-Jopeace, A.; Bryant, C. E.; Gay, N. J. The COP II adaptor protein TMED7 is required to initiate and mediate the delivery of TLR4 to the plasma membrane. *Sci. Signaling* **2014**, *7*, No. ra70.
(71) Fujita, M.; Watanabe, R.; Jaensch, N.; Romanova-Michaelides, M.; Satoh, T.; Kato, M.; Riezman, H.; Yamaguchi, Y.; Maeda, Y.; Kinoshita, T. Sorting of GPI-anchored proteins into ER exit sites by p24 proteins is dependent on remodeled GPI. *J. Cell Biol.* **2011**, *194*, 61−75.
(72) Tall, E.; Dormán, G.; Garcia, P.; Runnels, L.; Shah, S.; Chen, J.; Profit, A.; Gu, Q. M.; Chaudhary, A.; Prestwich, G. D.; Rebecchi, M. J. Phosphoinositide binding specificity among phospholipase C isozymes as determined by photo-cross-linking to novel substrate and product analogs. *Biochemistry* **1997**, *36*, 7239−7348.
(73) Bateman, A.; Martin, M. J.; Orchard, S.; et al. UniProt: the universal protein knowledgebase in 2021. *Nucleic Acids Res.* **2021**, *49*, D480−D489.

NOTE ADDED AFTER ASAP PUBLICATION

This paper was published online on January 26, 2023, with an error in the TOC/Abstract. The corrected version was reposted on February 6, 2023.

https://doi.org/10.1021/acs.jproteome.2c00728
J. Proteome Res. 2023, 22, 919−930